Linear Algebra and its Applications 431 (2009) 459–470

Contents lists available at ScienceDirect

Linear Algebra and its Applications

journal homepage: www.elsevier.com/locate/laa

A computational framework for image-based constrained registration[☆]

Eldad Haber [a,b], Stefan Heldmann [a], Jan Modersitzki [b,*]

[a] *Department of Mathematics and Computer Science, Emory University, Atlanta, GA, USA*
[b] *Department of Computing and Software, McMaster University, Hamilton, ON, Canada*

A R T I C L E I N F O

Article history:
Received 11 September 2008
Accepted 3 March 2009

Submitted by B. Fischer

This paper is dedicated to Sir Henk van der Vorst on the occasion of his 65th birthday

Keywords:
Image registration
Elastic matching
Constrained image registration
Local rigidity
Volume preserving registration

A B S T R A C T

Adding external knowledge improves the results for ill-posed problems. In this paper, we present a new computational framework for image registration when adding constraints on the transformation. We demonstrate that unconstrained registration can lead to ambiguous and non-physical results. Adding appropriate constraints introduces prior knowledge and contributes to reliability and uniqueness of the registration. Particularly, we consider recently proposed locally rigid transformations and volume preserving constraints as examples.

1. Introduction

Image registration is one of today's challenging problems in digital imaging. Roughly speaking, the problem is as follows: Given two images, find a *reasonable* spatial transformation such that a transformed version of the so-called template image, T, becomes *similar* to the so-called reference image R. Image registration is applied whenever images resulting from different times, devices, and/or perspectives need to be compared or integrated. It is used for example, in the evaluation of radiation therapy, surgery planning, estimation of treatment after cardiac arrest and more, see, e.g. [18,31,23,28,19] and references therein.

☆ This work is supported by NSF grant CCF-0427094 and DOE grant DE FG02-05ER25696.

* Corresponding author.
E-mail address: modersit@cas.mcmaster.ca (J. Modersitzki).

0024-3795/$ - see front matter © 2009 Elsevier Inc. All rights reserved.
doi:10.1016/j.laa.2009.03.020

As it is discussed in more details in Section 2, a registration procedure is typically based on two main building blocks. The first one is a distance measure that measures the similarity or proximity of images. A distance measure can be based on image features (e.g., landmarks or markers [3,27,34,28]), on image intensities (e.g., sum of squared differences, correlation, or mutual information [6,11,41]), on level sets [10,22], or on combinations hereof. For an overview and comparisons, see also [32,24,28]. The second building block is regularization. Since image registration is an ill-posed problem, regularization is inevitable and becomes a central topic [28]. There are two general approaches. In the first approach one restricts admissible transformations to a parametric model as, e.g., rigid or affine transformations (parameterized by rotation angles, scaling, and translations), or transformations that are linear combinations of a small set of basis functions (e.g. B-splines); see, e.g., [28] for an overview. It turns out that in many cases, this type of regularization is too restrictive and the desired transformation is not included in a parametric model. In these cases one has to turn to a more general regularization technique which is to add a penalty term to the objective function that outrules unwanted properties. This approach includes well-known regularizers such as the elastic [5], diffusion [13], or curvature [14] (and in a qualified sense also the fluid registration [8,4]); see also [28] for an overview. Fluid registration is in fact a flow approach, where the current configuration is updated in a regularized fashion. Other examples for flow approaches are Thirion's demons approach [38,40] or the diffeomorphic approaches [39,2,1,35] which restrict the transformation to be diffeomorphic.

Non-surprisingly and well-known, different regularizers can lead to highly different transformations as image registration is a highly ill-posed. The choice of regularization can have a key effect on the solution and its properties [28]. While choosing a regularization that fits a particular application is generally difficult, one can take measures to drastically reduce the level of non-uniqueness in the problem and thus make it less dependent on the particular regularization. One new and promising direction is to add physiologically meaningful constraints. Such constraints can be for example, incorporation of anatomical landmarks [12,9], rigidity of bones [36,26,29], or volume preservation of tumor tissue [33,21,20]. See also [15] for an overview. Note that diffeomorphic transformations do not necessarily fulfill any of these constraints, a trivial example is given by the diffeomorphism $\varphi(x) = 2x$.

Constraints can be added either as "hard"-constraints (i.e. the constraints have to be fulfilled exactly) or as "soft"-constraints (i.e. the constraints hold only approximately). As it is explained later, "soft"-constraints lead to a penalty approach which is known to be numerical untable or less efficient [30]. Therefore, this paper concentrates on "hard"-constraints.

Though it is very desirable to add constraints to the registration process, the computational framework for this incorporation is not well developed. This is especially the case for local constraints, where constraints are being applied on a small region within the image. There are two main difficulties in current methods for constrained image registration. First, all methods known to us are based on a Eulerian framework. While this approach is appropriate for the unconstrained case, problems may arise for the constrained case. In particular and as discussed in Section 2, the Eulerian approach generates non-differentiable constraints. Second, most of the current methods are based on a penalty approach, which leads to numerical ill-conditioning as well as inexact feasibility.

The goal of this paper is to propose a new computational framework for constrained image registration with emphasis on local constraints. Differentiability is maintained by using a Lagrangian framework and feasibility is obtained by using a Sequential Quadratic Programming (SQP) approach.

Moreover, the potential of the new framework is demonstrated by applying it to two important applications. The first application incorporates local rigidity; see also [25,26,37,29]. The second application integrates volume preservation; see also [33,20].

Incorporating constraints in registration is an important challenge. In contrast to choosing a particular regularization approach which is ad-hoc, image-based constraints are based on the physical attributes of the underlying image and therefore limit the optimization to physically feasible transformations.

The rest of the paper is structured as follows. In Section 2, we introduce the framework and form the mathematical setup. We show that superior numerical treatment can be given if we use a Lagrangian formulation to the problem. In Section 3, we discuss the examples of local rigidity and volume constraints. In Section 4, we suggest an SQP constrained optimization technique in order to solve the problem. In Section 5 we demonstrate the viability of our technique using synthetic models that highlight the advantages of our approach. Finally, we show the benefit of our approach for a clinical application.

2. Mathematical framework and problem description

In this section we formulate the constrained registration problem. Let $R, T \in L_2(\mathbb{R}^d; \mathbb{R})$ be two d-dimensional images. We want to find a transformation φ in some admissible functions space V such that the deformed template T is *similar* to R on a certain domain $\Omega \subset \mathbb{R}^d$. In particular, we only consider smooth and invertible transformations since we do not want cracks or folding in the deformed image. Therefore, the set of admissible functions contains only diffeomorphisms. While diffeomorphisms are commonly assumed for registration, we assume that additional information on φ is given. In particular, we assume a constraint on the transformation based on prior knowledge of the template image. Generally, such a constraint can be written as

$$\mathcal{C}(\varphi)(x) = 0 \quad \forall x \in \Sigma \subset \Omega.$$

That is, whenever we move a point, x in a certain sub-domain $\Sigma \subset \Omega$ the constraint applies to φ. For example, Σ can be obtained by the segmentation of the template image into rigid structures (bones in medical images) and therefore the constraint allows only rigid motion on Σ. Incompressible sub-structures present in the template image give another example for local constraints. Here, the Jacobian of transformation has to be one: $\det(\nabla\varphi(x)) = 1$ for $x \in \Sigma$.

It is also possible to add "soft"-constraints by using a penalty based on a semi-norm on $\mathcal{C}$. However, the penalty can be deduced from the "hard"-constraints [30], and we therefore focus on the latter.

Since the constraints apply only to a subset of the domain we use a regularized approach to compute a stable solution. To this end, we base our approach on constraint optimization where we minimize a functional build from of a distance measure $\mathcal{D}$ and a regularizer $\mathcal{S}$. That is, we compute a transformation that minimizes $\mathcal{D} + \alpha\mathcal{S}$ subject to the given constraints, where $\alpha > 0$ is the regularization parameter. For clarity of presentation, we particularly consider the sum of squared differences (SSD) for the distance measure and an L_2-norm based regularizer $\mathcal{S}$, where with a differential operator $\mathcal{B}$,

$$\mathcal{S}(\varphi) := \|\mathcal{B}\varphi\|^2_{L_2(\Omega)}.$$

The above description of our approach is still not specific enough. Before we give an exact mathematical formulation we have to decide about a transformation model. Generally, we have the Eulerian or Lagrangian frameworks, see also Fig. 1.

Let φ be a transformation that moves a point $x \in \Omega$ to $y = \varphi(x)$. Since we consider invertible transformations, this is equivalent to arriving at point y from $x = \psi(y)$, where for ease of presentation $\psi = \varphi^{-1}$. Let us consider the pair of a point x and the function value $T(x)$. In the so-called Lagrangian framework we consider the forward transform φ. Here, $(x, T(x))$ is moved and *arrives at* $(y, T(x)) = (\varphi(x), T(x))$ from $x \in \Omega$. Alternatively, in the Eulerian framework we fix the location in the deformed image. Here, at a fixed point $y \in \Omega$ in the deformed image the point is *arriving from*

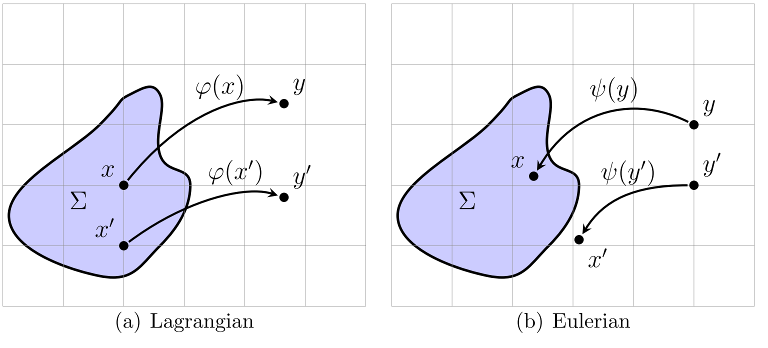

Fig. 1. The Lagrangian approach (a): grid point x in Σ maps to non-grid point $y = \varphi(x)$. The Eulerian approach (b): a grid point y is mapped from the non-grid point $x = \psi(y)$, where $\psi = \varphi^{-1}$. (a) Lagrangian (b) Eulerian.

point $x = \psi(y)$ such that the deformed image at y is given by $(y, T(x)) = (y, T(\psi(y))$ for $y \in \Omega$. The two concepts are illustrated in Fig. 1.

It is important to note that constraints on the transformation are often modeled in the Lagrangian framework, i.e., usually we pose constraints on the forward transform φ rather than ψ (as we did in the above examples). Therefore, when using the Eulerian framework we have to find an equivalent expression for the constraints. Formally, having a constraint

$$\mathcal{C}^L(\varphi)(x) = 0 \quad \text{for all } x \in \Sigma \tag{1}$$

on φ in the Lagrangian framework, we have to find an equivalent formulation $\mathcal{C}^E(\psi)$ that holds for all $x = \psi(y) \in \Sigma$. Thus, (1) can be expressed in the Eulerian approach as

$$\mathcal{C}^E(\psi)(y) = 0 \quad \text{for all } \psi(y) \in \Sigma. \tag{2}$$

The crucial difference between both approaches is that in the Lagrangian framework the points where the constraint is active depend on Σ alone while in the Eulerian framework they depend on Σ *and* φ. A typical remedy is to trace the indicator function for Σ. However, this results in a non-differentiable constraint.

Since it provides some computational advantages for unconstrained applications, most often the Eulerian framework is used for registration. However, it turns out that when adding constraints it becomes more difficult. Therefore, we propose using the Lagrangian framework in the constrained setting. Next, we explore the difference between the Eulerian and Lagrangian approaches.

2.1. Constraint registration within the Eulerian framework

In the Eulerian framework, we compare a point $(y, R(y))$ of the reference image to $(y, T(\psi(y))$ for $y \in \Omega$, where again $\psi = \varphi^{-1}$. For example, the standard SSD distance measure for this setting is given by

$$\mathcal{D}^E(\psi) := \frac{1}{2}\int_{\Omega} (T(\psi(y)) - R(y))^2 \, dy, \tag{3}$$

and the constrained image registration problem in Eulerian framework reads

$$\begin{array}{ll} \text{Find } \psi \text{ such that} & \mathcal{D}^{\text{SSD}}(\psi) + \alpha\mathcal{S}(\psi) = \min \\ \text{subject to} & \mathcal{C}^E(\psi)(y) = 0 \quad \text{for all } \psi(y) \in \Sigma. \end{array} \tag{4}$$

The problem with the Eulerian approach is that the domain in which the constraints are active needs to be tracked; see also [29]. This implies that the constraints are not differentiable with respect to ψ in general. Fig. 1 (right) presents an intuitive explanation. Considering the point y' and $x' = \psi(y')$, where x' is outside but arbitrarily close to Σ. As long as x' is outside Σ the constraint is inactive. However, a small change of ψ can bring x' inside and the constraint becomes active. This implies that the constraint is not differentiable with respect to ψ. Since in the Eulerian framework ψ is precisely the quantity to look at, computational problems are to be expected.

To explain the above point a bit more formally we use the characteristic function $\chi_\Sigma(x)$ and rewrite the Eulerian constraint $\mathcal{C}^E(\psi)(y) = 0$ for $\psi(y) \in \Omega$ as

$$\chi_{\psi(\Sigma)}(y)\, C^E(\psi)(y) = 0 \quad \text{for all } y \in \Omega.$$

Then clearly, the non-differentiability of the indicator function yields non-differentiable constraints in the usual way. One could still work with the interface and use an approximation to the delta function as derivatives but this is rather complicated [29]. Next we see that a much simpler treatment can be obtained by considering the Lagrangian approach.

2.2. Constraint registration within the Lagrangian framework

The problem of non-differentiable constraints and constraint-tracking leads us to use the Lagrangian approach. In the Lagrangian framework, we consider the forward transform φ. Here, $(x, T(x))$ gets moved to $(y, T(x)) = (y, T(\varphi^{-1}(y)))$ for all $x \in \Omega$ or equivalently for all $y \in \varphi(\Omega)$. For example, the SSD distance measure for this setting is given by

$$\frac{1}{2}\int_{\varphi(\Omega)}\left(T(\varphi^{-1}(y))-R(y)\right)^2\,dy.$$

First we note that, with changing φ we also change the domain of integration. This is a problem, since if a transformation shrinks Ω, the above distance is reduced. To prevent this, we consider an averaged distance

$$\frac{1}{2}\frac{1}{|\varphi(\Omega)|}\int_{\varphi(\Omega)}\left(T(\varphi^{-1}(y))-R(y)\right)^2\,dy \quad \text{where } |\varphi(\Omega)|:=\int_{\varphi(\Omega)}dx.$$

On first view, this expression seems to have two major drawbacks. First it depends on both φ and φ^{-1}. Second, the domain of integration also depends on φ. This is probably the reason for the popularity of the Eulerian approach for unconstrained registration. However, changing variables to $x=\varphi^{-1}(y)$ and using the transformation rule, we find

$$\int_{\varphi(\Omega)}\left(T(\varphi^{-1}(y))-R(y)\right)^2\,dy=\int_{\Omega}(T(x)-R(\varphi(x)))^2\,|\det\nabla\varphi(x)|\,dx$$

and $|\varphi(\Omega)|=\int_{\Omega}|\det\nabla\varphi(x)|\,dx$. Therefore, we define

$$\mathcal{D}^L(\varphi):=\frac{1}{2}\left(\int_{\Omega}|\det\nabla\varphi(x)|\,dx\right)^{-1}\int_{\Omega}(T(x)-R(\varphi(x)))^2\;|\det\nabla\varphi(x)|\,dx. \tag{5}$$

Clearly, this distance measure is more involved than $\mathcal{D}^E$ in the Eulerian framework. However, the main point is that this approach is better suited for the constraints. To see that, we rewrite the problem in the Lagrangian framework

$$\begin{array}{ll}\text{Find } \varphi \text{ such that} & \mathcal{D}^L(\varphi)+\alpha\mathcal{S}(\varphi)=\min\\ \text{subject to} & \mathcal{C}^L(\varphi)(x)=0 \quad \text{for all } x\in\Sigma.\end{array} \tag{6}$$

In particular, the constraint domain does not have to be tracked and thus, the constraint is differentiable with respect to φ, assuming differentiability of $\mathcal{C}^L$ with respect to φ.

To demonstrate the above points we next consider two applications, the local rigidity and volume constraints. Using these constraints as model problem, we demonstrate the application of the constraints in the Lagrangian framework and subsequently its numerical treatment.

3. Constraints

3.1. Rigidity constraints

Human anatomy presents a couple of visible compartments in most image modalities, such as air, blood, bone, CFS, fat, or muscle. Probably the most obvious constraint is to maintain the rigidity of bones. Consider the illustrative example presented in Fig. 2, where a simplified model of a knee is being registered to a bent model using elastic registration. Using an unconstrained approach, the grid shows some highly non-physical deformations in areas one would expect the transformation to be rigid. To overcome such difficulties we add local rigidity constraints that allow for a much more realistic deformation. It is important to stress that the resulting images of the constrained and unconstrained approach are almost identical though the deformations are very different.

Since a 2D rigid transformation can be phrased as $Q(\theta)x+b$, where $b\in\mathbb{R}^2$ denotes the translation, and

$$Q(\theta)=\begin{pmatrix}\cos\theta & \sin\theta\\ -\sin\theta & \cos\theta\end{pmatrix},$$

the rotation matrix, the local rigidity constraint in the Lagrangian framework can be written as

$$\mathcal{C}^L(\varphi)(x)=\mathcal{C}^L(\varphi,\theta,b)(x)=\varphi(x)-(Q(\theta)x+b)=0 \quad \text{for all } x\in\Sigma. \tag{7}$$

This constraint is nonlinear with respect to rotation angles θ but linear with respect to the translation b and transformation φ. Furthermore, it is important to note that if $\Sigma=\Sigma_1\cup\cdots\cup\Sigma_M$ is

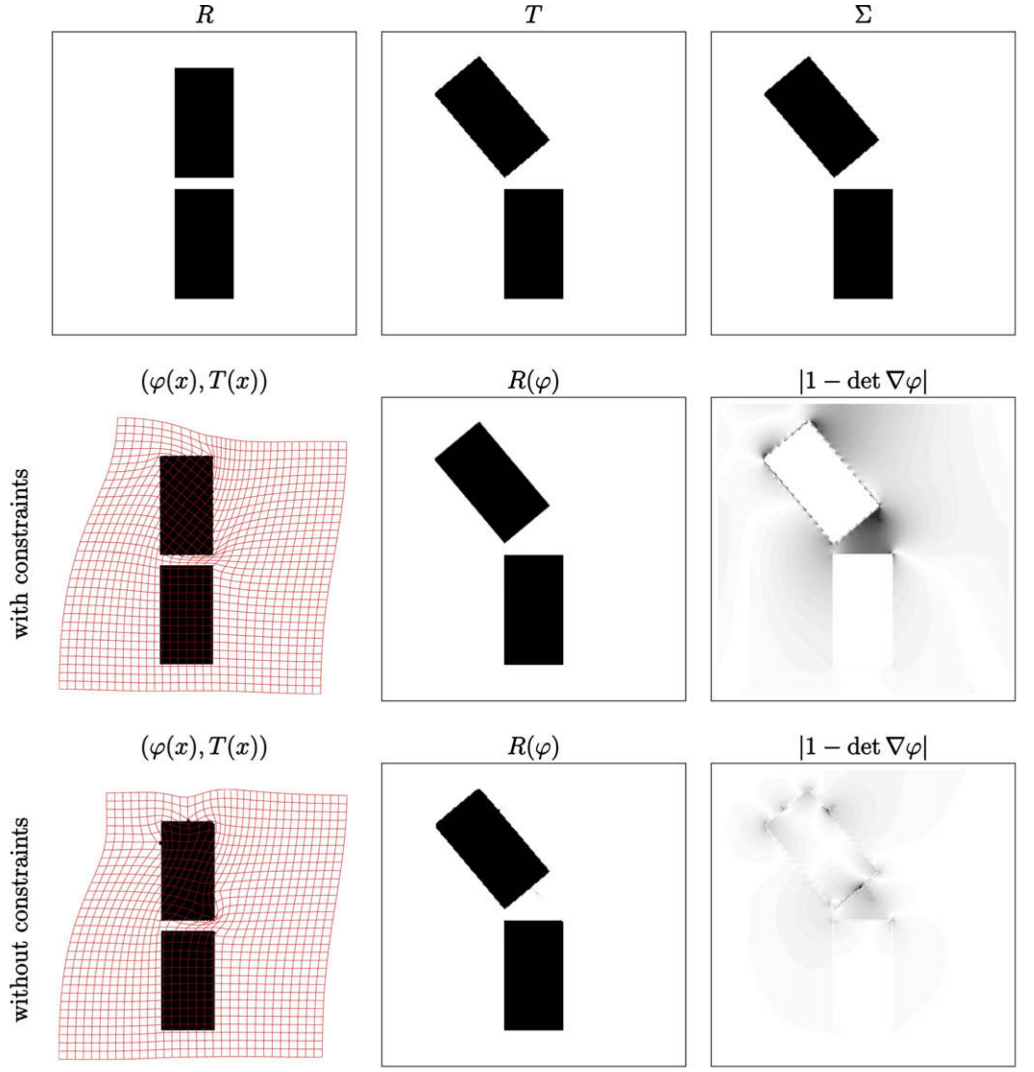

Fig. 2. Registration results for a synthetic knee; the top row shows the reference, template, and a segmentation for the rigid structures in the template. The constrained and unconstrained results are shown in second and third row, from left to right: the transformed template (Lagrangian view) with a visualization of the transformation, the transformed reference (Eulerian view), and a map of the volume change.

composed of several disjoint domains Σ_k we need a set of parameters (θ_k, b_k) for each domain to allow for independent rigid motion. In this case, we can write (7) as

$$\mathcal{C}^L(\varphi, \theta_k, b_k)(x) = 0 \quad \text{for all } x \in \Sigma_k \text{ and } k = 1, \ldots, M.$$

For ease of presentation, we drop the dependence on k. The local rigidity constrained registration is to solve the following problem:

$$\begin{array}{ll} \text{Find } \varphi, \theta, b \text{ such that} & \mathcal{D}^L(\varphi) + \alpha\mathcal{S}(\varphi) = \min \\ \text{subject to} & \mathcal{C}^L(\varphi, \theta, b)(x) = 0 \quad \text{for all } x \in \Sigma. \end{array} \tag{8}$$

In this particular case,

$$y = \varphi(x) = Q(\theta)x + b \Leftrightarrow x = \psi(y) = Q(\theta)^\top(y - b) = Q(\hat{\theta})y + \hat{b}$$

setting $\hat{\theta} = -\theta$ and $\hat{b} = -Q(\hat{\theta})b$. Thus, the nature of the constraints $\mathcal{C}^L$ and $\mathcal{C}^E$ for the Lagrangian and Eulerian framework coincides and the Eulerian version of (8) reads:

$$\begin{array}{ll} \text{Find } \psi, \hat{\theta}, \hat{b} \text{ such that} & \mathcal{D}^E(\psi) + \alpha\mathcal{S}(\psi) = \min \\ \text{subject to} & \mathcal{C}^E(\psi, \hat{\theta}, \hat{b})(y) = 0 \quad \text{for all } \psi(y) \in \Sigma, \end{array}$$

where $\mathcal{C}^E(\psi, \hat{\theta}, \hat{b})(y) = \mathcal{C}^L(\psi, \hat{\theta}, \hat{b})(y) = \psi(y) - (Q(\hat{\theta})y + \hat{b})$. However, even in this case of basically identical constraints for both frameworks, the problems of non-differentiability and constraint-tracking in the Eulerian approach remain and cause major computational problems. Before presenting our Lagrangian based computational approach, local volume preserving constraints are considered.

3.2. Volume preserving constraints

A typical task for image registration is the combination complementary information from several images. For example in multi-phase CT imaging when a contrast agent is used for the visualization of vessels and blood-flow or to compare pre-and-post treatment of tumors. In such cases, one would like to register the images without changing the volume of some of the structure, like tumors.

If unconstrained registration is performed, volume of tumors is changed if this reduces the objective function. To prevent such phenomena we add volume preservation as a local constraint. To this end we use a segmentation to identify a set Σ of points where the transformation has to preserve volume. Formally, we explicitly require that

$$|S| = |\varphi(S)| \quad \text{for all subsets } S \subset \Sigma, \tag{9}$$

where $|\varphi(S)| := \int_{\varphi(S)} dx$ and $|S| := \int_S dx$. Furthermore, after changing variables we find

$$\varphi(S)| = \int_{\varphi(S)} dx = \int_S |\det \nabla\varphi|\, dx$$

and hence (9) is equivalent to $\det \nabla\varphi = 1$ on Σ. Therefore, the volume preservation constraint in the Lagrangian framework can be defined as

$$\mathcal{C}^L(\varphi)(x) = \det \nabla\varphi(x) - 1 = 0 \quad \text{for all } x \in \Sigma. \tag{10}$$

This constraint is highly nonlinear and involves the product of the derivatives of the transformation φ. For consistent discretization of this constraint we point to [20]. The discretization of these constraints yields a highly nonlinear set of equations that need to be solved in the course of the solution of the registration.

4. Numerical approaches for constrained image registration

We now discuss a general framework to solve the constrained optimization problem posed in the Lagrangian framework.

Considering (8) as model problem, we seek a transformation φ which solves the following discretized constrained optimization problem:

$$\text{Minimize } J(\varphi) := D(\varphi) + \alpha S(\varphi) \quad \text{subject to } C(\varphi) = 0, \tag{11}$$

where D, S, C are discretized versions of $\mathcal{D}, \mathcal{S}, \mathcal{C}$, and with abuse of notation we use the same symbol φ for a discrete grid function of the continuous deformation.

We propose to use two different optimization frameworks. First, we discuss the use of Sequential Quadratic Programming (SQP). Second, in the particular case of the rigidity constraints where $C = C(\varphi, \theta, b)$, we are able to eliminate the constraints.

4.1. Optimization via SQP

In the SQP framework Newton's method is used in order to find a stationary point of the Lagrangian

$$\mathcal{L}(\varphi,\theta,b,\lambda) = J(\varphi) + \lambda^\top C(\varphi,\theta,b),$$

where λ is a vector of Lagrange multipliers. That is, one needs to solve the nonlinear system $\nabla\mathcal{L} = 0$, i.e.,

$$\begin{aligned}&\nabla J(\varphi) + \nabla C(\varphi,\theta,b)^T\lambda = 0,\\ &C(\varphi,\theta,b) = 0.\end{aligned} \tag{12}$$

At each iteration the linearization of (12) is solved for updates $\delta\varphi$, $\delta\theta$, δb, $\delta\lambda$ of our variables, that is

$$\begin{pmatrix} H & \nabla C^\top \\ \nabla C & 0 \end{pmatrix}\begin{pmatrix}\delta\tilde{\varphi}\\ \delta\lambda\end{pmatrix} = -\begin{pmatrix}\nabla J + \nabla C^\top\lambda \\ C\end{pmatrix}, \tag{13}$$

where H is an approximation to the Hessian $\nabla^2\mathcal{L}$ and $\delta\tilde{\varphi} = (\delta\varphi,\delta\theta,\delta b)^\top$. In standard line search SQP methods the variables are updated using a line search that guarantees a sufficient reduction in some merit function. To be more specific, we seek to decrease the non-differentiable L_1 merit function

$$\mathrm{merit}(\varphi,\theta,b;\mu) = J(\varphi) + \mu\|C(\varphi,\theta,b)\|_1,$$

where μ is a parameter which needs to be chosen judicially [30].

Recent developments in SQP algorithms are described in [17,7,16]. The major difficulty when applying SQP methods to constrained image registration is that a reasonably accurate solution of the linear sub-problem in (13) is required for most algorithms. Since the system is large and indefinite we use an iterative Krylov solver (MINRES) for the solution of the system with block preconditioning; see [20] for details on solving the linear system.

4.2. Optimization via constraint elimination

In some cases such as rigidity constraints, the constraints are simple enough such that we can consider a simple elimination of the constraints. Consider first the case of a single domain Σ where the displacement is rigid. In this case we can divide the displacement vector into two parts. The first part, φ_0 is the part that is outside Σ and the second, φ_1 is the part that belongs to Σ. Thus we can rewrite the displacement vector as

$$\varphi = \begin{pmatrix}\varphi_0\\ \varphi_1\end{pmatrix} = \begin{pmatrix}\varphi_0\\ Q(\theta)x + b\end{pmatrix}.$$

In the case that we have more than a single domain of rigidity we rewrite the displacement vector as

$$\varphi = \begin{pmatrix}\varphi_0\\ \varphi_1\\ \cdots\\ \varphi_M\end{pmatrix} = \begin{pmatrix}\varphi_0\\ Q(\theta_1)x + b_1\\ \cdots\\ Q(\theta_M)x + b_M\end{pmatrix}.$$

Substituting φ in the objective function we obtain an unconstrained optimization problem. We then use the Gauss–Newton method for the solution of the optimization problem.

5. Numerical experiments

We present results from three experiments that demonstrate the importance of rigidity and volume constraints. The first two experiments are academic in nature and the third is a realistic difficult knee registration. For all experiments we use the elastic regularizer and compare the results for the constrained and unconstrained approach. For the rigidity constrained registration we used the method where we eliminated the constraints while for the volume constrained registration we used SQP. All images considered are 2D and have a size of 256×256 pixels.

In the first experiment we explore a synthetic knee model where two blocks are deformed; cf. Fig. 2. A direct comparison of the constrained and unconstrained approach is presented. Though the transformed images are very similar, the transformations are very different: the constrained approach preserves the rigid structures.

In the second experiment we use MRI images of a knee. We use manual segmentation to obtain the bones; cf. Fig. 3. Again, we see that when constraints are not present, non-physical results are obtained. An important difference to the academic examples above is that not only the transformation but also the transformed image are different. Moreover, the unconstrained approach fails and does not give a meaningful result. Therefore, adding the constraints is substantial to obtain a reasonable solution.

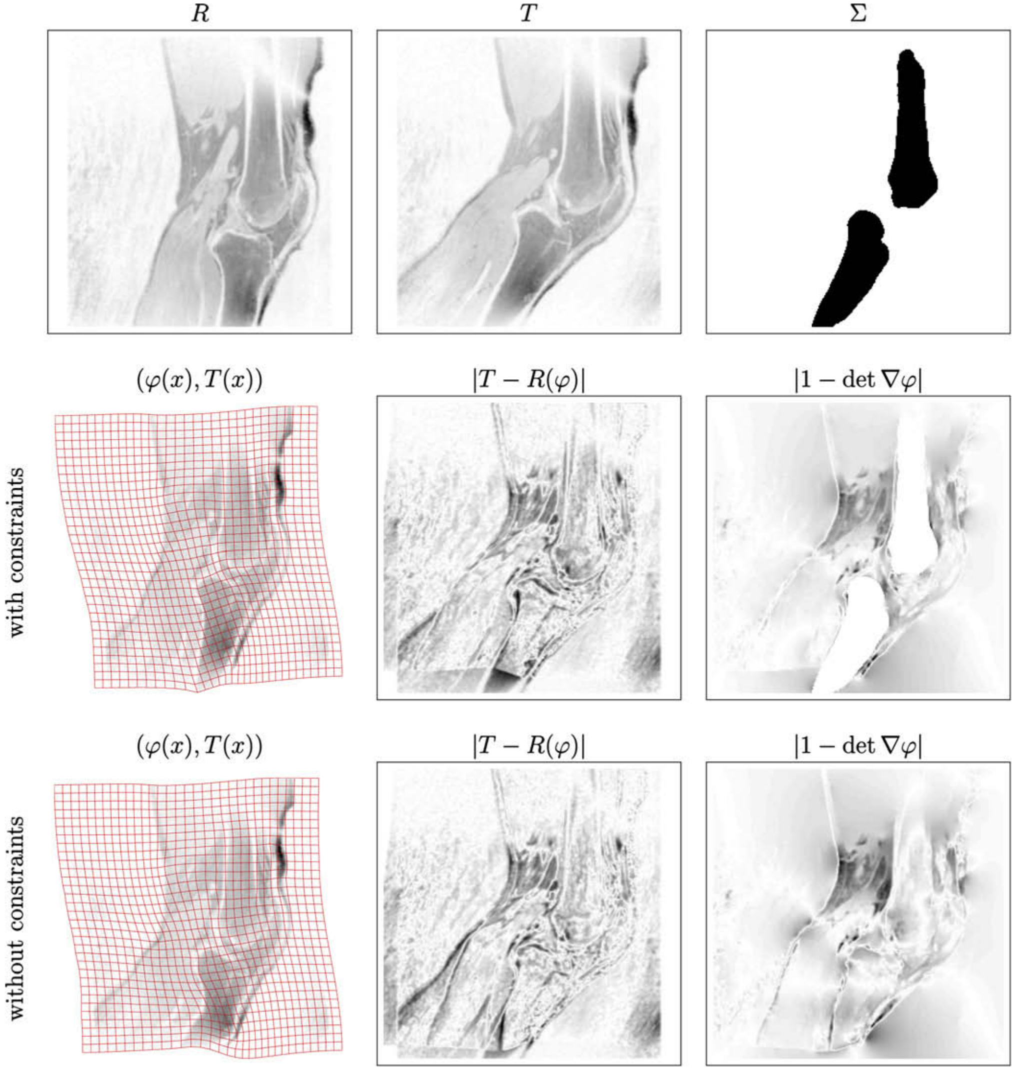

Fig. 3. Registration results for human knee images; the top row shows the reference, template, and a segmentation for the rigid structures in the template. The constrained and unconstrained results are shown in second and third row in the Lagrangian view; from left to right: the transformed template with a visualization of the transformation, the difference between template and transformed reference, and a map of the volume change.

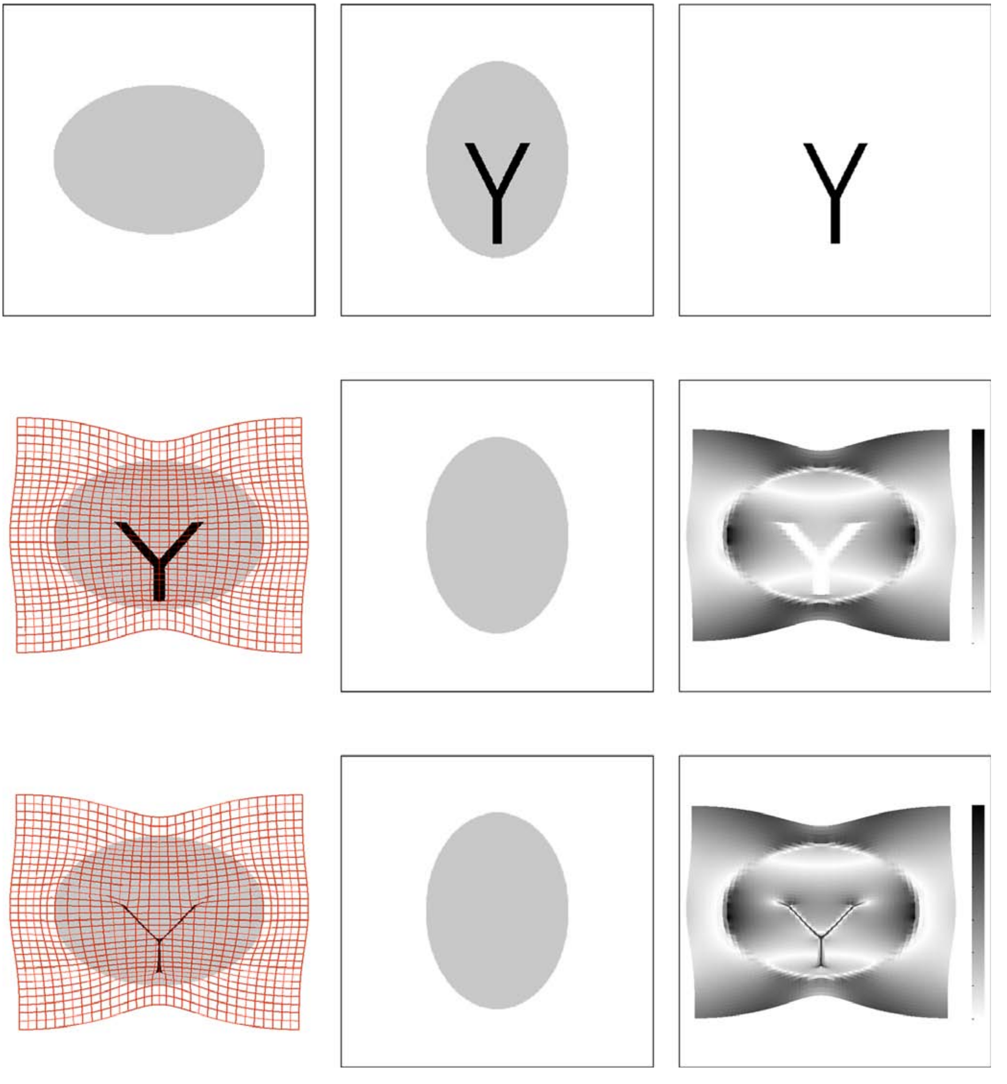

Fig. 4. Registration results for artificial images; the top row shows the reference, template, and a segmentation for the rigid structures in the template. The constrained and unconstrained results are shown in second and third row, from left to right: the transformed template (Lagrangian view) with a visualization of the transformation, the transformed reference (Eulerian view), and a map of the volume change.

We emphasis that the constrained approach does not necessarily yield the "true" solution. However, since we assume that some structure do transform rigidly, we know that the unconstrained approach yields a non feasible result. In this sense, the constrained approach is more reliable than the unconstrained approach.

In our third experiment we use a synthetic example of the deformation of two ellipses, one with a *Y*-structure embedded in it (see Fig. 4). When no constraints are present, the *Y* tends to shrink. This helps to reduce the distance measure and thus reduces the objective function. This result is not realistic as we do not expect the *Y* structure to disappear. When the volume constraint is added, the ellipses fit without changing the volume of the *Y*.

Table 1
Computation results for the unconstrained Eulerian approach and the constrained Lagrangian framework.

Problem	Constraints	CPU time
Synthetic knee	X	40.8s
Synthetic knee	✓	57.9 s
Real knee	X	220.1 s
Real knee	✓	240.5 s
Synthetic Y	X	220.1 s
Synthetic Y	✓	240.5 s

Using the Lagrangian framework with constraints adds to the computational cost. We have additional computational costs from the Jacobian in distance measure (5) and the constraints (6) compared to an unconstrained approach in the Eulerian framework; cf. (3) and (4). However, we found the increase of computations is moderate. To give a rough idea, the computation times of the three different experiments for the constrained approach in the Lagrangian framework and corresponding unconstrained methods in the Eulerian framework are summarized in Table 1. Comparing the computational work, we see that using constraints adds roughly 15% of computational time compared with the unconstrained approach. Thus, adding constraints increases the computational work but gives more reliable results.

6. Conclusions

In this paper we have developed a framework for local constrained image registration and applied it to rigidity and volume constraints. There are a few features that distinguish our method compared to others. In particular

- The proposed method uses constraints rather than a penalty and therefore the constraints are actually fulfilled. Also, using constrained optimization does not require choosing a penalty parameter.
- We use the Lagrangian approach. This saves the need to track the domain of the constraints but adds the cost of computing the determinant of the Jacobian.
- Generally, sequential quadratic programming can be used for solving the constrained optimization problem.
- As a particular example, we examined rigidity and volume constraints. We have found that the increase of computations stayed moderate with approximately 15% compared to a unconstrained approach.

Numerical experiments show that adding constraints can increase the reliability of non-parametric registration and reduce the inherent non-uniqueness of the problems. We therefore advocate that adding constraints will become common practice in image registration.

References

[1] B.B. Avants, P.T. Schoenemann, J.C. Gee, Lagrangian frame diffeomorphic image registration: morphometric comparison of human and chimpanzee cortex, Medical Image Anal. 10 (2006) 397–412.
[2] F. Beg, M. Miller, A. Trouvé, L. Younes, Computing large deformation metric mappings via geodesic flows of diffeomorphisms, IJCV 61 (2005) 139–157.
[3] F.L. Bookstein, Principal warps: thin-plate splines and the decomposition of deformations, IEEE PAMI 11 (1989) 567–585.
[4] M. Bro-Nielsen, Medical Image Registration and Surgery Simulation, Ph.D. Thesis, IMM, Technical University of Denmark, 1996.
[5] C. Broit, Optimal Registration of Deformed Images, PhD thesis, Computer and Information Science, University of Pensylvania, 1981.
[6] L.G. Brown, A survey of image registration techniques, ACM Comput. Surveys 24 (1992) 325–376.
[7] R.H. Byrd, M.E. Hribar, J. Nocedal, An interior point algorithm for large scale nonlinear programming, SIAM J. Optim. 9 (4) (2000) 877–900.
[8] G.E. Christensen, Deformable Shape Models for Anatomy, Ph.D. Thesis, Sever Institute of Technology, Washington University, 1994.

[9] G.E. Christensen, H.J. Johnson, Consistent image registration, IEEE TMI 20 (2001) 568–582.
[10] U. Clarenz, M. Droske, M. Rumpf, Towards fast non-rigid registration, in: Inverse Problems, Image Analysis and Medical Imaging, AMS Special Session Interaction of Inverse Problems and Image Analysis, vol. 313, AMS, 2002, pp. 67–84.
[11] A. Collignon, F. Maes, D. Delaere, D. Vandermeulen, P. Suetens, G. Marchal, Automated multi-modality image registration based on information theory, in: IPMI, 1995, pp. 263–274.
[12] B. Fischer, J. Modersitzki, Fast inversion of matrices arising in image processing, Numer. Algorithms 22 (1999) 1–11.
[13] B. Fischer, J. Modersitzki, Fast diffusion registration, AMS Contemp. Math., Inverse Problems, Image Anal., Med. Imaging 313 (2002) 117–129.
[14] B. Fischer, J. Modersitzki, Curvature based image registration, J. Math. Imaging Vision 18 (2003) 81–85.
[15] B. Fischer, J. Modersitzki, Ill-posed medicine – an introduction to image registration, Inverse Problems 24 (2008) 1–19–2023.
[16] R. Fletcher, S. Leyffer, User manual for filter SQP, Numerical Analysis Report NA/181, Dundee University, April 1998.
[17] R. Fletcher, S. Leyffer, P.L. Toint, On the global convergence of a filter-sqp algorithm, SIAM J. Optim. 13 (n1) (2002) 44–59.
[18] C. Glasbey, A review of image warping methods, J. Appl. Statist. 25 (1998) 155–171.
[19] A.A. Goshtasby, 2-D and 3-D Image Registration, Wiley Press, New York, 2005.
[20] E. Haber, J. Modersitzki, Numerical solutions of volume preserving image registration, Inverse Problems 20 (2004) 1621–1638.
[21] E. Haber, J. Modersitzki, Image registration with a guaranteed displacement regularity, IJCV 1 (2006), doi: 10.1007/s11263-006-8984-4.
[22] E. Haber, J. Modersitzki, Intensity gradient based registration and fusion of multi-modal images, Methods Inform. Med., Schattauer Verlag, Stuttgart 46 (2007) 292–299.
[23] J. Hajnal, D. Hawkes, D. Hill, Medical Image Registration, CRC Press, 2001.
[24] G. Hermosillo, C. Chefd'hotel, O. Faugeras, Variational methods for multimodal image matching, IJCV 50 (2002) 329–343.
[25] J. Little, D. Hill, D. Hawkes, Deformations incorporating rigid structures, Comput. Vision Image Understanding 66 (1997) 223–232.
[26] D. Loeckx, F. Maes, D. Vandermeulen, P. Suetens, Nonrigid image registration using free-form deformations with a local rigidity constraint, in: Medical Image Computing and Computer-Assisted Intervention – MICCAI 2004, vol. 3216/2004, 2004, pp. 639–646.
[27] C.R. Maurer, J.M. Fitzpatrick, Interactive image-guided neurosurgery, Park Ridge, IL, American Association of Neurological Surgeons, 1993, pp. 17–44 (ch. A Review of Medical Image Registration).
[28] J. Modersitzki, Numerical Methods for Image Registration, Numerical Mathematics and Scientific Computation, Oxford University Press, 2003.
[29] J. Modersitzki, FLIRT with rigidity – image registration with a local non-rigidity penalty, IJCV (2008) 153–163, doi: 10.1007/s11263-007-0079-3.
[30] J. Nocedal, S. Wright, Numerical Optimization, Springer, New York, 1999.
[31] J. Pluim, J. Maintz, M. Viergever, Mutual-information-based registration of medical images: a survey, IEEE TMI 22 (1999) 986–1004.
[32] A. Roche, Recalage d'images mé par infé statistique, Ph.D. thesis, Université de Nice, Sophia-Antipolis, France, 2001.
[33] T. Rohlfing, C.R. Maurer Jr., D.A. Bluemke, M.A. Jacobs, Volume-preserving nonrigid registration of MR breast images using free-form deformation with an incompressibility constraint, IEEE TMI 22 (2003) 730–741.
[34] K. Rohr, Landmark-based Image Analysis, Computational Imaging and Vision, Kluwer Academic Publishers, Dordrecht, 2001.
[35] D. Rueckert, P. Aljabar, R.A. Heckemann, J. Hajnal, A. Hammers, Diffeomorphic registration using b-splines, in: Ninth International Conference on Medical Image Computing and Computer-Assisted Intervention (MICCAI 2006), October 2006.
[36] M. Staring, S. Klein, J.P.W. Pluim, A rigidity penalty term for nonrigid registration, Med. Phys. 34 (2007) 4098–4108.
[37] M. Staring, S. Klein, J.P.W. Pluim, Nonrigid registration using a rigidity constraint, in medical imaging 2006: image processing, in: J.M. Reinhardt, J.P.W. Pluim (Eds.), Proceedings of the SPIE, vol. 6144, March 2006, pp. 355–364.
[38] J.-P. Thirion, Non-rigid matching using demons, in: CVPR'96: Proceedings of the 1996 Conference on Computer Vision and Pattern Recognition (CVPR'96), 1996, p. 245.
[39] A. Trouvé, Diffeomorphisms groups and pattern matching in image analysis, IJCV 28 (1998) 213–221.
[40] T. Vercauteren, X. Pennec, A. Perchant, N. Ayache, Non-parametric diffeomorphic image registration with the demons algorithm, in: MICCAI 2007, Brisbane, 2007, pp. 319–326.
[41] P. Viola, W.M. Wells, Alignment by maximization of mutual information, IJCV 24 (1997) 137–154.